Terahertz Terabit Wireless Communication

Kao-Cheng Huang and Zhaocheng Wang

Kao-Cheng Huang (kch@ieee.org) is with Dharma Academy, Taiwan. Zhaocheng Wang (zcwang@mail.tsinghua.edu.cn) is with the Department of Electronic Engineering, Tsinghua University, Beijing 100084, P.R. China.

Digital Object Identifier 10.1109/MMM.2011.940596
Date of publication: 5 May 2011

Recently, terahertz (THz) technology has attracted a great deal of interest from academia and industry. This is due to a number of interesting features of THz waves, including the tens and hundreds of gigahertz bandwidths available, and the fact that this frequency band poses only a minor health threat. Also, as millimeter-wave communication systems mature [1], [2], the focus of research is, naturally, moving to the THz range. According to Shannon theory [3], the broad bandwidth of the THz frequency bands can be used for terabit-per-second (Tb/s) wireless indoor communication systems (see "Terabit Versus Terahertz"). This enables several new applications, such as cordless phones with 360° autostereoscopic displays, optic-fiber replacement, and wireless Tb/s file transferring. All of these applications provide higher quality and a better user experience. Although THz technology could satisfy the demand for an extremely high data rate, a number of technical challenges need to be overcome or better understood before its development.

This article provides an overview the state-of-the-art in THz wireless communication and it is also a tutorial for an emerging application in Terabit radio systems. The objective is to construct robust, low-cost wireless systems for THz terabit communications.

Terahertz Wave Propagation

To design THz wireless communications, the first step is to investigate THz wave propagation characteristics in free space and then to conduct channel measurements. The main issue for THz wave propagation is atmospheric attenuation, which is dominated by water vapor absorption in the THz frequency band. From experiments on the propagation of THz waves in air, it is observed that there are a number of THz transmission windows [4]. (The frequency ranges between two water vapor absorption peaks are THz transmission windows.) Nine major transmission windows throughout the 0.1–3 THz frequency range are indicated and can be used for wireless communications. The nine major THz transmission bands are

- 0.1−0.55 THz
- 0.56−0.75 THz
- 0.76–0.98 THz
- 0.99−1.09 THz
- 1.21−1.41 THz
- 1.42−1.59 THz
- 1.92−2.04 THz
- 2.05−2.15 THz
- 2.47−2.62 THz [5].

Terabit Versus Terahertz

Shannon's ideal communication theorem is expressed as

$$C = B \cdot \log_2(1+\mathrm{S/N}) \quad \text{unit: b/s,}$$

where C is called the "channel capacity" in bits per second (b/s). This represents the maximum error-free communication rate for a communication channel having bandwidth B and signal-to-noise power ratio of S/N. Hence, in theory, it is possible to convey information at a rate of up to C with no errors in the received message at all. In order to support 1 Tb/s transmission under the constraint of a reasonable signal-to-noise ratio limit, the minimum required bandwidth is around 0.2 THz. This indicates that only THz frequency range could provide this kind of available spectrum and enable high-rate communications beyond 1 Tb/s.

Figure 1 illustrates the THz spectra after different propagation distances in the atmosphere. The transmission bands become narrower as the propagation distance increases. Reasonable bandwidths remain, however, even when the propagation distance reaches 108 m. The attenuation below 0.65 THz is from beam divergence due to diffraction, not from the atmosphere [6].

Terahertz Wave Transmitters

When a THz transmitter (Tx) that utilizes binary-frequency-shift keying (FSK) is considered, it is vital to have a controllable THz source (see "FSK Modulator"). Various methods for generating THz waves have been thoroughly studied throughout the last decade. In general, there are two types of THz signaling protocols that can be used for wireless communications: continuous-wave (CW) and pulsed signals.

This article could not exhaustively cover all of the detailed aspects of THz signal generation and detection techniques such as black-body radiation [7], free-electron laser [8], and p-Ge emitter. Instead, the following material only reviews THz techniques that are affordable and feasible for THz communication systems.

Continuous-Wave Signal Generation from Photomixers

Photomixing process is commonly used to generate THz CWs from two CW laser beams. We define that these lasers have angular frequencies ω_1 and ω_2,

To design THz wireless communications, the first step is to investigate THz wave propagation characteristics in free space and then to conduct channel measurements.

respectively. Both beams with the same polarization are mixed and then focused onto an ultrafast semiconductor material. Due to the photonic absorption and the short charge carrier lifetime in the material, we obtain the modulation of the conductivity at the expected THz frequency $\omega_{THz} = \omega_1 - \omega_2$. Figure 2(a) schematically shows the two-beam photomixing with a photomixer coupled to a hemispherical substrate lens. Figure 2(b) shows a schematic diagram of the photoconductive emitter and an identical detector.

Low-temperature-grown GaAs (LT-GaAs) is a widely used substrate for the photomixer. Its unique properties include a short carrier lifetime [around 0.5 picosecond (ps)], a large breakdown-field threshold (greater than 300 kV/cm), and a relatively high carrier mobility (approximately 200 $cm^2V^{-1}s^{-1}$), each of which is vital for the efficiency of the photomixing process. The photomixing efficiency can be enhanced by reducing the transit time of majority carriers to much less than 1 ps in photomixers and photodetectors [9]. Output CW power is in the range of 0.1–5 μW, depending on pump power and operating frequency [15].

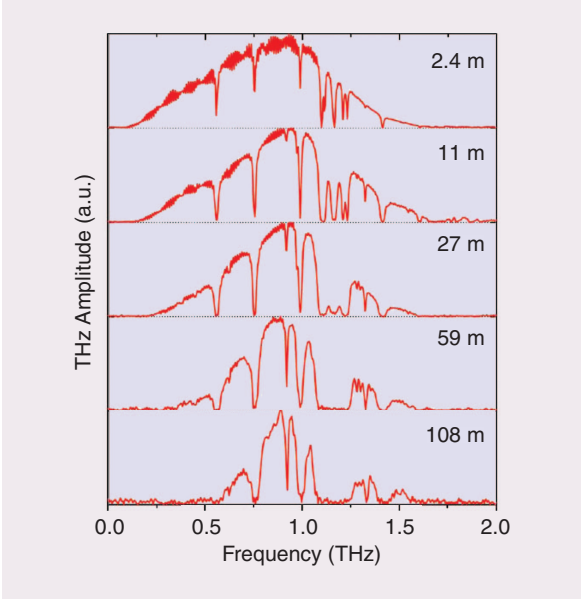

Figure 1. *Terahertz spectra at different propagation distances under free space, line-of-sight conditions. The temperature of measurements is 22 °C, and the relative humidity is about 10% [6].*

FSK Modulator

In a general FSK modulator, the rectangular bit stream 01001..11010 is transformed to levels +/1 and is sent to the modulator. At the modulator, one frequency corresponds to level +1, and another one to level −1. In this case we have the classical FSK modulated signal.

Pulse Generation (Optical Method)

The optical generation method uses a laser with a pulse width of 10–200 femtosecond (fs), which is in the visible or infrared spectrum. This laser is pointed at a THz-generating medium, (e.g., dielectric crystals, semiconductors, organic materials). Semiconductors can be advantageous for generating THz pulses with high spectral intensity at higher THz frequencies. $LiNbO_3$ is better suited to generate THz pulses that have a very large relative spectral width.

Optical rectification is a second-order phenomenon (difference frequency mixing) in a nonlinear medium with large second-order susceptibility. The difference between optical rectification and photoconduction is

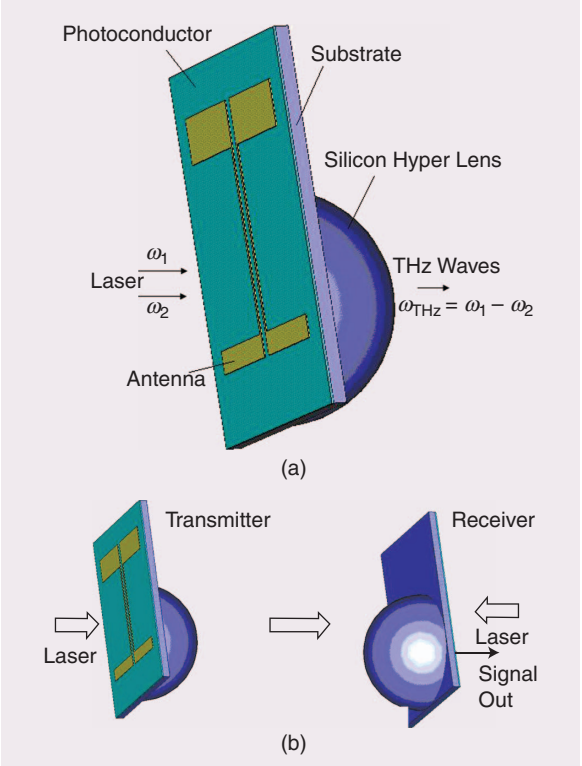

Figure 2. *(a) A schematic view of two-beam photomixing with a photomixer, which couples to a silicon hemispherical lens. The incident angular frequencies are ω_1 and ω_2, respectively. The output terahertz frequency ω_{THz} is the difference between ω_1 and ω_2. (b) A schematic diagram of the photoconductive emitter and identical detector along with a typical free-space terahertz system incorporating lenses. The same arrangement can be applied to both pulsed and continuous-wave based terahertz communication systems.*

TABLE 1. Terahertz wave generation.

Technology	Power	Tunability	Coherence/ Stability	Affordability/ Availability	Misc.	Ref.
Blackbody radiation	Poor	Good	Poor	Good	$f > 5$ THz	[7]
Free-electron laser	Excellent	Excellent	Good	Bad	Very wideband	[8]
Photomixer	Fair	Good	Very good	Fair	$f < 3.8$ THz Tunable, CW	[9]
Laser pulse excited THz generation	Fair	Fair	Fair	Poor	Good at higher f	[10], [11]
Monolithic nonlinear transmission lines	Fair	Fair	Good	Good	$f < 1$ THz	[11]

that the visible exciting beam creates virtual carriers rather than real ones. Thus, the transmission result in rectification produces THz radiation, while both reflection and transmission results in photoconduction to generate THz radiation. The output power of the photoconduction process can be increased with higher pump power. The photoconductive sources are capable of relatively large average THz powers of 100 μW [12]. The average power of optical rectification is of the order of μW range (e.g., 35–60 μW THz power generation with the use of a pulsed laser oscillator at 160−260 mW output power). As optical rectification relies on relatively low efficiency coupling of the incident optical power to THz frequencies, it generally provides lower output powers than photoconductive antennas. On the other hand, optical rectification attracts much attention to generate 0.1–5 THz for its simplicity and spectral broadness [13].

Pulse Generation (Electronic Method)

An all-electronic system uses monolithic nonlinear transmission lines as ultrafast voltage-step generators. The nonlinear transmission lines may be used for both generating picosecond pulses and for driving monolithically integrated diode samplers for the detection of these pulses.

The nonlinear transmission lines method, shown in Figure 3, is a transmission line that is periodically loaded with reverse-biased Schottky varactor diodes, serving as voltage-variable capacitors. This causes a wave traveling along the line to experience a voltage-dependent propagation velocity, resulting in a shock wave whose main features resemble a step function.

The advantages of this approach lie in its low phase noise, low cost, relative simplicity, and robustness. The disadvantage is its limited available frequency range, which is below 1 THz. The average output power level is on the order of −10 dBm [11]. Based on the previous THz wave propagation discussion, nonlinear transmission lines can be applied to the first four transmission windows: 1) 0.1–0.55 THz, 2) 0.56–0.75 THz, 3) 0.76–0.98 THz, and 4) 0.99–1.09 THz for wireless communications.

Terahertz Wave Detectors/Receivers

To detect THz pulse signals, the waves first are focused on a detector or a photoconductive antenna. The double refraction of a silicon lens [Figure 2(a)] or an electro-optic crystal can be read using a probe pulse, usually split up from the laser used in THz generation. The probe beam is then measured with a quarter-wavelength plate. Finally, the time delay between the probe pulse and the THz signal can be measured to obtain the electric field in the time domain.

Photoconductive Antennas

Photoconductive antennas (see Figure 4) are widely used for effective THz detection as well as for emission and are commonly made from either silicon or GaAs. Laser pulses, separated from the pump laser, probe the antenna. To determine the THz waveform, the time delay from pump and probe pulses is measured as well as the change in dc current from the antenna [14].

The antenna in Figure 4 is built with a GaAs substrate, but other semiconductors, such as GaSe, may also be used. The gap in the middle is biased by a dc voltage, A, and is probed by laser pulses split off from

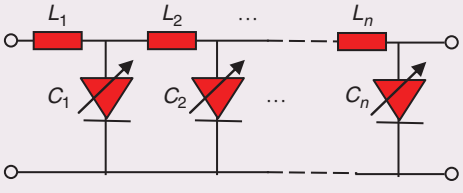

Figure 3. *Nonlinear transmission line method. The configuration is a transmission line (with inductors L_1, L_2, …) periodically loaded with reverse-biased Schottky varactor diodes. The diodes, serving as voltage-variable capacitors (C_1, C_2, …), cause a wave to travel along the line.*

The photomixer has the advantage of being able to synchronize multiple devices located at distant places via the fiber-optic network.

the laser pump in the case of detection. The gap is about 8 μm. The width of the antenna is approximately 15 μm, and the length is about 40 μm (see Figure 4). The THz waves strike the antenna which, in turn, causes slight transient current changes [14]. The bandwidth of the antenna is affected by several key factors: the duration of the laser pulse, the physical structure of the antenna, the carrier scattering time, and the THz beam optics [14].

Photomixers with Bulk Structures

Semiconductor photomixers with bulk structures provide wide optical bandwidths over 1 THz, but they suffer from narrow electrical bandwidths [16]. One solution is to apply a tunable local oscillator (LO); this allows us to develop a sensitive heterodyne receiver (Rx). In the Rx, the incoming THz signal is mixed with the LO signal and down-converted to the intermediate frequency (IF) signal. The sensitivity of the Rx is determined by the ratio of the IF signal power to the system noise power. The mixer is saturated by the LO power before reaching the quantum-noise limit, and the sensitivity is limited by the mixer/amplifier noise. In certain cases, the saturation behavior is important for the Rx to avoid a change in sensitivity caused by LO-power fluctuations.

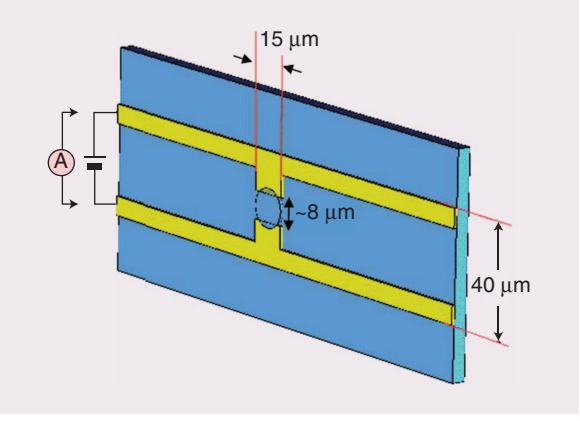

Figure 4. *Photoconductive antenna structure (not to scale).*

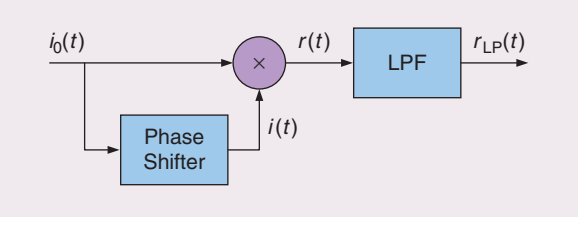

Figure 5. *A basic model of a differential detector.*

The photomixer has the advantage of being able to synchronize multiple devices located at distant places via the fiber-optic network. It can also be applied to a wireless metropolitan area network where optical links are established.

Monolithic Microwave Integrated Circuit Method

The design and characterization of a 0.22 THz microstrip single-chip Rx has been demonstrated with an integrated antenna in a 100 nm GaAs metamorphic high-electron-mobility-transistor (mHEMT) technology [16]. This mHEMT THz Rx has two advantages: broad operating frequency bandwidth and low noise figure. This Rx's performance is superior to the latest results presented using CMOS or SiGe technology. Also, this technology enables low-cost solutions when compared to pure Indium Phosphide (InP)-substrate-based designs. The THz Rx monolithic microwave integrated circuit (MMIC) consists of a silicon substrate lens fed antenna, a low-noise amplifier, and a subharmonically pumped resistive mixer. The double sideband noise figure of this quasi-optical Rx is as low as 8.4 dB (1750 K) at 220 GHz, including the losses in the antenna and in the silicon lens [16], [17].

Low-Power Design Without Mixer and Local Oscillator

For pulse-generated signals, a simple diode detector is preferred due to cost considerations. Alternatively, to demodulate CW-based binary FSK transmitted signals, a differential detector without an LO is used (detailed in Figure 5) [1]. This Rx consists of a phase shifter, mixer, and low-pass filter. The input signal, $i_0(t)$, is supplied to both the phase shifter and the mixer. The phase shifter shifts the phase at the carrier frequency of the input signal $i_0(t)$ by $-\pi/2 \pm 2N\pi$, where N is an integer, and outputs a phase-shifted signal $i(t)$ to the mixer. The mixer multiplies the input signal $i_0(t)$ by the phase-shifted signal $i(t)$ and outputs a down-converted signal $r(t)$ to the low-pass filter. In the THz frequency range, though, it is challenging to implement the mixer module in Figure 6 as the wavelength is very short so its phase tuning in small scale is unstable using conventional methods.

A balanced detector without a complex mixer has been proposed, as depicted in Figure 6(a). It comprises three adders, two square-law detectors, a phase shifter, and a low-pass filter. An input signal $i_0(t)$ is supplied to the phase shifter and the adders A and B. The phase shifter shifts the phase of the input signal and outputs

a shifted signal $i(t)$ to the adders A and B. The adder A adds the input signal $i_0(t)$ and the shifted signal $i(t)$ generated by the phase shifter and outputs the resulting signal to the first square-law detector. By squaring the output signal from the adder A, the first square-law detector presents the first squared signal $r_1(t)$ to the adder C. In contrast, the adder B subtracts the input signal $i_0(t)$ from the shifted signal $i(t)$ generated by the phase shifter and outputs the resulting signal to the second square-law detector. Similarly, by squaring the output signal from the adder B, the second square-law detector presents the second squared signal $r_2(t)$ to the adder C. The adder C then subtracts the second squared signal $r_2(t)$ from the first squared signal $r_1(t)$, respectively, and passes the combined signal $r(t)$ to the low-pass filter.

The layout of the balanced differential detector as shown in Figure 6(b) is designed by scaling down all aspects of microstrip technology. The length difference between curves a and b operates as the phase shifter in Figure 6(a). They are designed to adjust phase difference to be $-\pi/2 \pm 2N\pi$. The outputs connect to the square-law detectors in Figure 6(a).

It is clear that both detectors from Figure 5 and Figure 6 are mathematically identical. Since simple diodes are adopted instead of the complex mixer, the balanced differential detector is low-profile for THz wireless communications.

Terahertz Transistors

From the perspective of cost-effectiveness and communication quality, transistors operating at THz frequenies are desirable for constructing practical communication systems (e.g., balanced differential detector, etc.). We thus briefly review the present situation of THz transistors in this section. The development of THz transistor includes the following approaches:

1) Heterojunction bipolar transistor (HBT) with transit frequency (f_T) ~ 0.8 THz was reported [18]. The electrical properties of InP materials clearly offer performance possibilities that greatly exceed those of SiGe. The InP HBT technology focused on a scaled emitter width of 300 nm tailored for high frequency gain. Measurements indicate that the technology is capable of achieving maximum oscillation frequency (f_{max}) > 0.5 THz, making it suitable for switches, phase shifters, amplifiers, oscillator design at THz frequencies [19].
2) High-electron mobility transistors (HEMTs) with $f_{max} > 1.0$ THz was reported [20]. Going forward, THz Electronics will attempt to drive InP HEMT technology to 20 nm gate lengths and demonstrate $f_T > 1.2$ THz and $f_{max} > 2.25$ THz. These frequencies will be accessible through the reduction of internode capacitances C_{gs} to below 0.4 pF/mm and source resistance $R_{source} < 0.1\ \Omega \cdot$ mm.

Ballistic deflection transistor (BDT) is a six-terminal coplanar structure etched into a two-dimensional electron gas.

3) Ballistic deflection transistor (BDT) is a six-terminal coplanar structure etched into a two-dimensional electron gas. In the BDT, the steering voltage is much smaller than that required for gate pinch-off, which, combined with the reduced gate capacitances of the two-dimensional electron gas (2DEG), results in an estimated f_T in the THz range with low noise and low power consumption at room temperature [21].
4) Nanowire field-effect transistors (NWFETs) were firstly reported in the sub-100-nm Ge/Si channel length regime. When channel length is reduced to 70 nm, THz intrinsic operation speed is possible. In addition to transistors, it is also possible to use crossbar nanowire circuits to make nonvolatile switch devices and synthetically coded nanowire for multiplexing/demultiplexing [22].

Challenges in System Issues

Modern THz communication systems are dedicated to consumer electronics applications and, therefore, must

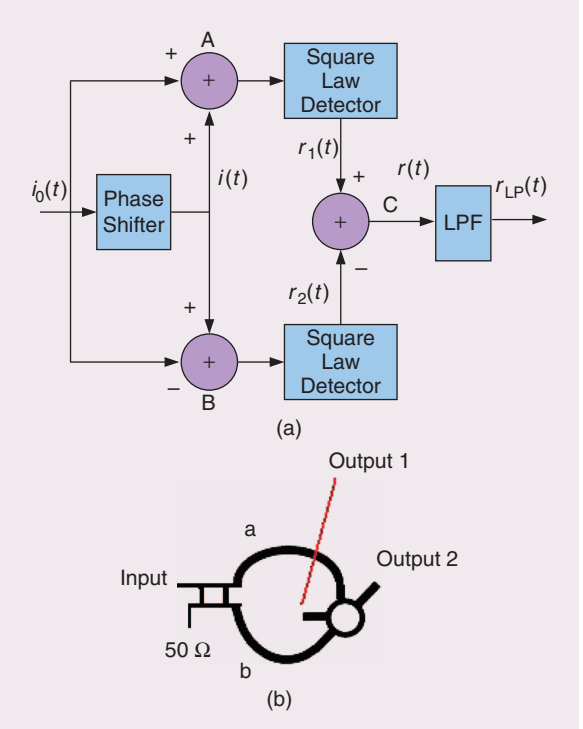

Figure 6. *(a) A balanced differential detector without using a mixer and a local-oscillator. (b) An example of layout (not to scale). Two outputs connect to the square-law detectors in (a).*

From the perspective of cost effectiveness and communication quality, transistors operating at THz frequencies are desirable for constructing practical communication systems.

meet strict requirements, including small size, light weight, and low production cost. Moreover, there are numerous challenging constraints on antenna design, such as high gain (>20 dBi) and wide bandwidth (>90° half-power beam width), while maintaining a small size [1].

To build a THz link, a single microstrip antenna is not enough, as it has low antenna gain and narrow impedance bandwidth. Also, because of the high water/air attenuation at THz frequencies, the transmitting power should be increased, and the receiving noise should be minimized. We can either improve the power amplifier or use an antenna with 20 dBi gain or above. In general, THz power amplifiers consume high dc power, so a high-gain antenna is more cost effective. It is strongly recommended to apply lens antennas or phased-array antennas to amplify line-of-sight received signals and minimize interference [23].

When a narrow-beam antenna is adopted for both the Tx and the Rx, beam directions from both sides are rotated either mechanically or electrically in order to find the strongest wireless link based on the measured channel quality information. During the rotation, the half-power beam width of the main beam, or the main radiation pattern, is kept unchanged. The algorithm to control the rotation and to handle the coordination between the Tx and the Rx and successfully exchange the control signaling is called "beam steering." After beam steering, the strong line-of-sight (LOS)/non-LOS (NLOS) paths can be aligned and the link budget requirements can be satisfied due to the inherent antenna gain from both narrow-beam antennas.

If a phased-array antenna is used, one should consider the trade-off between the antenna size and the losses due to the long feed network. One example of phased-array antennas is shown in Figure 7. From the Tx side, the baseband and RF signal are identical for all the patch antenna elements. The coefficients W_i for $i = 1, \ldots, M$ are adjusted to realize beam forming,

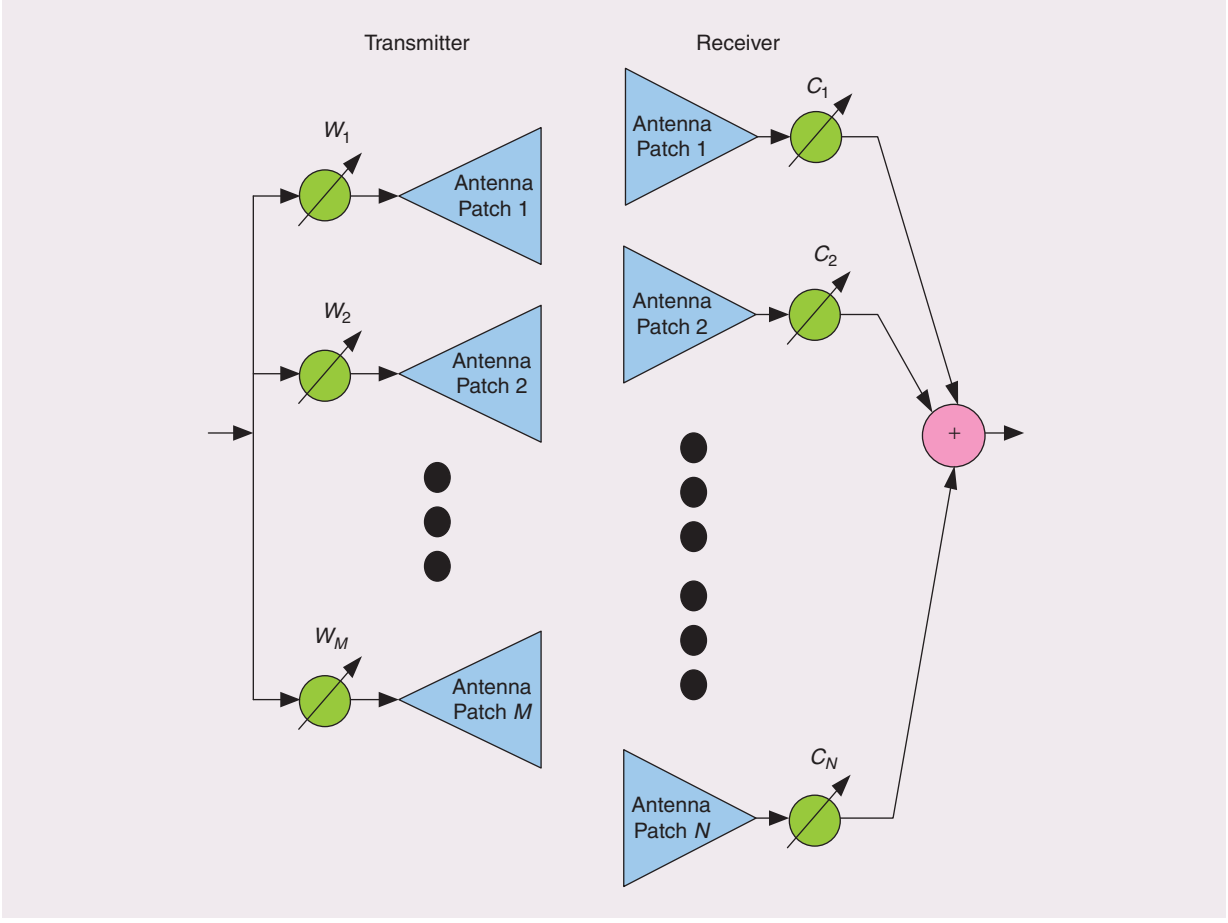

Figure 7. *System model of phased-array antennas.*

where the coefficient amplitude for each patch element can be changed and its corresponding phase can be shifted. For THz circuits, the feed loss of phased-array antennas is relatively high. To improve the performance, each patch antenna could have its own embedded power amplifier to reduce the effect of the feed loss.

From the Rx side, the multiple received RF signals are then combined from all of the patch antenna elements. The coefficients Ci for $i = 1, \ldots, N$ are adjusted to obtain the maximum received signal-to-noise ratio (SNR), whereby the amplitude of the coefficient for each patch element can be changed and its corresponding phase can be shifted. Similar to the Tx, each patch element could have its own embedded low-noise amplifier before the combiner to reduce the effect of the feed loss and fulfill the strict link budget requirements.

At the Tx side, multiple phase shifters receive the output from the mixer that is working at the THz range. A demultiplexer is included to control which phase shifters receive the signal. These phase shifters are either quantized phase shifters or complex multipliers. The phase and/or magnitude of the currents in each patch element are adjusted to produce a desired beam pattern, as illustrated in Figure 8. The beam pattern may neither be symmetric nor have only one main lobe (i.e., regular beam); an irregular beam pattern with multiple main lobes is produced in order to maximize the received SNR under dynamic wireless conditions.

With respect to the Rx side, a phased-array antenna with multiple patch elements receives the signals and then sends them to the phase shifters having different coefficients As discussed previously, phase shifters comprised either quantized phase shifters or complex multipliers. The phase shifters receive the signals from antennas, which are then combined to form a single output, as shown in Figure 7. A multiplexer is used to combine the signals from the different elements and to output the combined signal through the single feed line. As mentioned previously, the phases and magnitudes of the patch elements in the phased-array antennas are adjusted to produce a desired beam pattern, as illustrated in Figure 8. Additionally, the beam pattern may have more than one strong beam direction. An irregular beam pattern is generated to maximize the received SNR.

The success of the THz radio will largely depend on the advancement of THz front end, THz transistors, and the development of advanced system concepts.

From a design point of view, complex multipliers are difficult to implement for THz circuits. Quantized phase shifters with very limited amplitude or phase selections are preferred, especially for millimeter-wave and submillimeter-wave-based applications [24]. As we have emphasized above, the idea of beam forming is not concentrated on the search for an antenna radiation pattern having a good shape but instead is concentrated on maximizing the received SNR under a dynamic wireless environment. The corresponding antenna radiation patterns from both Tx and Rx sides might have strange beam shapes, which are illustrated in Figure 8.

Conclusion

Different aspects of Tb/s radios working in the THz frequency range have been discussed. It is encouraging to see the advancements in technology development with respect to these radios. The characteristics of THz

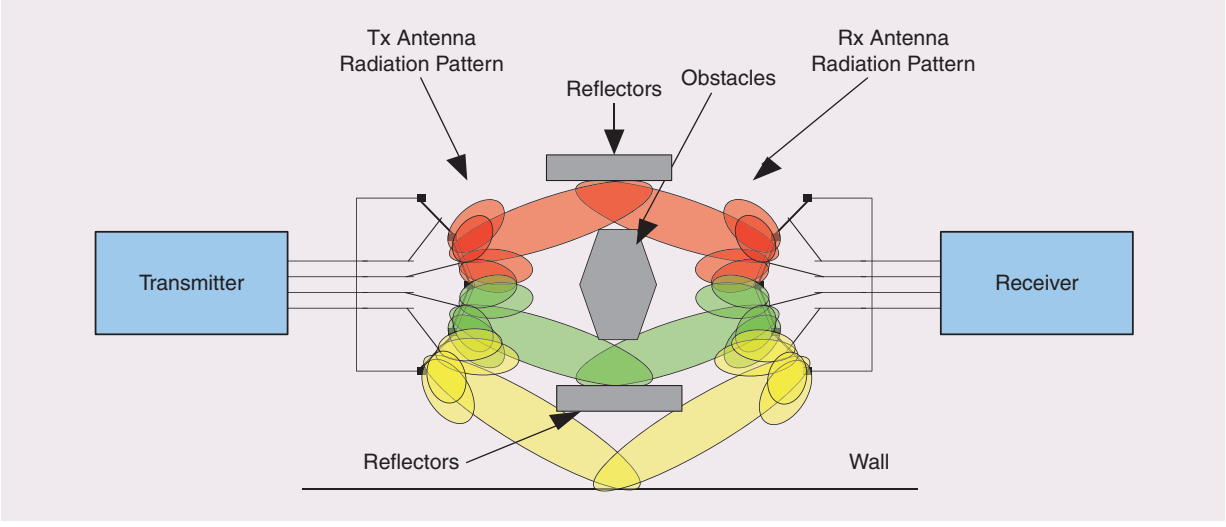

Figure 8. *One example of a phased-array antenna with an irregular antenna radiation pattern.*

Semiconductors can be advantageous for generating THz pulses with high spectral intensity at higher THz frequencies.

propagation in free space were first summarized. Provided that the requisite bandwidth is available, FSK can satisfy the required performance with a simpler, lower-cost transceiver configuration. Technically, the success of the THz radio will largely depend on the advancement of THz front end, THz transistors, and the development of advanced system concepts. Different THz generating and detecting methods were reviewed and compared. In particular, a novel FSK Rx with no mixer and no LO was described for THz wireless applications. It has the benefits of minimizing power consumption and simplifying the circuit configuration. An example of layout is given. Finally, a new system concept was discussed with irregular antenna radiation patterns on both the Tx and Rx sides to establish an adaptive Tb/s wireless link. The techniques discussed are intended to provide an efficient means to complete a first-order assessment of the options available to system designers and also to narrow the choices to those that provide adequate performance and less cost. This article provides a preliminary study on the state of the art of the THz Tb communications. The conceptual framework of these systems is still in the research phase, not yet ready for practical use.

Acknowledgment

The authors would like to thank Hsiang-Jung Huang for her assistance.

References

[1] K. Huang and Z. Wang, *Millimeter Wave Communication Systems* (IEEE Series on Digital & Mobile Communication). Hoboken: Wiley-IEEE Press, 2011.

[2] R. C. Daniels, J. N. Murdock, T. S. Rappaport, and R. W. Heath, "60 GHz wireless: Up close and personal," *IEEE Microwave Mag. Suppl.*, vol. 11, no. 7, pp. 544–550, Dec. 2010.

[3] R. E. Miles, P. Harrison, and D. Lippens, *Terahertz Sources and Systems*, 1st ed. Berlin, Germany: Springer-Verlag, 2001.

[4] J. F. O'Bryon, *Assessment of Millimeter-Wave and Terahertz Technology for Detection and Identification of Concealed Explosives and Weapons*. Washington, DC: National Academies Press, 2007.

[5] T. Seta, J. Mendrok, and Y. Kasai, "Laboratory spectroscopic measurement of water vapor for the terahertz-wave propagation model," in *Proc. URSI Chicago General Assembly*, Aug. 2008, pp. 1–4.

[6] H. Liu, H. Zhong, N. Karpowicz, Y. Chen, and X. Zhang, "Terahertz spectroscopy and imaging for defense and security applications," *Proc. IEEE*, vol. 95, no. 8, pp. 1514–1527, 2007.

[7] T. Hofmann, U. Schade, C. M. Herzinger, P. Esquinazi, and M. Schubert, "Terahertz magneto-optic generalized ellipsometry using synchrotron and blackbody radiation," *Rev. Sci. Instrum.*, vol. 77, no. 6, pp. 1–12, 2006.

[8] E. L. Saldin, E. V. Schneidmiller, and M. V. Yurkov, *The Physics of Free Electron Lasers*. New York: Springer-Verlag, 2000.

[9] S. Pilla, "Enhancing the photomixing efficiency of optoelectronic devices in the terahertz regime," *Appl. Phys. Lett.*, vol. 90, no. 16, pp. 1–3, 2007.

[10] T. M. Antonsen, J. Palastro, A. York, S. Varma, H. Milchberg, and J. Cooley, "THZ generation by ultra-short laser pulses propagating in nonuniform plasma channels," in *Proc. 33rd IEEE Int. Conf. Rec. Plasma Science*, Traverse City, MI, 2006, pp. 372.

[11] D. Weide, "Applications and outlook for electronic terahertz technology," *Optics Photonics News*, vol. 14, no. 4, pp. 48–53, 2003.

[12] D. Creeden, J. C. McCarthy, P. A. Ketteridge, P. G. Schunemann, T. Southward, J. J. Komiak, and E. P. Chicklis, "Compact, high average power, fiber-pumped terahertz source for active real-time imaging of concealed objects," *Opt. Express*, vol. 15, no. 10, pp. 6478–6483, 2007.

[13] G. Andrei, J. H. Stepanov, and K. Jürgen, "Efficient generation of subpicosecond terahertz radiation by phase-matched optical rectification using ultrashort laser pulses with tilted pulse fronts," *Appl. Phys. Lett.*, vol. 83, no. 15, pp. 3000–3002, 1983.

[14] M. Tani, M. Herrmann, and K. Sakai, "Generation and detection of terahertz pulsed radiation with photoconductive antennas and its applications to imaging," *Meas. Sci. Technol.*, vol. 13, no. 11, pp. 1739–1745, 2002.

[15] K. Sakai, *Terahertz Optoelectronics*, 1st ed. New York: Springer-Verlag, 2005.

[16] S. E. Gunnarsson, N. Wadefalk, J. Svedin, S. Cherednichenko, I. Angelov, H. Zirath, I. Kallfass, and A. Leuther, "A 220 GHz single-chip receiver MMIC with integrated antenna," *IEEE Microwave Guided Wave Lett.*, vol. 18, pp. 284–286, Apr. 2008.

[17] S. Koch, M. Guthoerl, I. Kallfass, A. Leuther, and S. Saito, "A 120–145 GHz heterodyne receiver chipset utilizing the 140 GHz atmospheric window for passive millimeter-wave imaging applications," *IEEE J. Solid-State Circuits*, vol. 45, no. 10, pp. 1961–1967 Oct. 2010.

[18] W. Snodgrass, W. Hafez, N. Harff, and M. Feng, "Pseudomorphic InP/lnGaAs heterojunction bipolar transistors (PHBTs) experimentally demonstrating ft = 765 GHz at 25 °C increasing to ft = 845 GHz at −55 °C," in *Proc. IEEE Int. Electron Devices Meeting*, Dec. 2006, pp. 1–4.

[19] J. D. Albrecht, M. J. Rosker, H. B. Wallacet, and T. Chang, "THz electronics projects at DARPA: Transistors, TMICs, and amplifiers," in *IEEE MTT-S Int. Microwave Symp. Dig.*, May 2010, pp. 1118–1121.

[20] R. Lai, X.B. Mei, W.R. Deal, W. Yoshida, Y.M. Kim, P.H. Liu, J. Lee, J. Uyeda, V. Radisic, M. Lange, T. Gaier, L. Samoska, and A. Fung, "Sub 50 nm InP HEMT device with Fmax greater than 1 THz," in *IEEE Int. Electron Devices Meeting Dig.*, Dec. 2007, pp. 609–611.

[21] Q. Diduck, M. Margala, and M. J. Feldman, "A terahertz transistor based on geometrical deflection of ballistic current," in *IEEE MTT-S Int. Microwave Symp. Dig.*, June 2006, pp. 345–347.

[22] Y. A. Tarakanov and J. M. Kinaret, "A carbon nanotube field effect transistor with a suspended nanotube gate," *Nano Lett.*, vol. 7, no. 8, pp. 2291–2294, 2007.

[23] J. Thornton and K. Huang, *Modern Lens Antennas for Communications Engineering* (IEEE Series on Electromagnetic Wave Theory). Hoboken: Wiley-IEEE Press, to be published.

[24] *CoMPA (Consortium of Millimeter Wave Practical Applications) Proposal*, IEEE Standard 802.15-07-0693-01-003c, May 2007.